Role of the 5′ TAR Stem−Loop and the U5-AUG Duplex in Dimerization of HIV-1 Genomic RNA†

Rujun Song, Jafar Kafaie, and Michael Laughrea*

McGill AIDS Center, Lady Davis Institute for Medical Research, Jewish General Hospital, Montreal, Quebec, Canada H3T 1E2, and Department of Medicine, McGill University, Montreal, Quebec, Canada H3A 2B4

Received November 23, 2007; Revised Manuscript Received December 28, 2007

ABSTRACT: The HIV-1 genome consists of two identical RNAs that are linked together through noncovalent interactions involving nucleotides from the 5′ untranslated region (5′ UTR) of each RNA strand. The 5′ UTR is the most conserved part of the HIV-1 RNA genome, and its 335 nucleotide residues form regulatory motifs that mediate multiple essential steps in the viral replication cycle. Here, studying the effect of selected mutations both singly and together with mutations disabling SL1 (SL1 is a 5′ UTR stem−loop containing a palindrome called the dimerization initiation site), we have done a rather systematic survey of the 5′ UTR requirements for full genomic RNA dimerization in grown-up (i.e., predominantly ≥10 h old) HIV-1 viruses produced by transfected human and simian cells. We have identified a role for the 5′ transactivation response element (5′ TAR) and a contribution of a long-distance base pairing between a sequence located at the beginning of the U5 region and nucleotides surrounding the AUG Gag initiation codon. The resulting intra- or intermolecular duplex is called the U5-AUG duplex. The other regions of the 5′ UTR have been shown to play no systematic role in genomic RNA dimerization, except for a sequence located around the 3′ end of a large stem−loop enclosing the primer binding site, and the well-documented SL1. Our data are consistent with a direct role for the 5′ TAR in genomic RNA dimerization (possibly via a palindrome encompassing the apical loop of the 5′ TAR).

In all grown-up retroviruses, the genome consists of two identical RNAs linked together by noncovalent interactions (*1*). [In newly released viruses, the genome can appear substantially monomeric (*1*).] A dimeric genomic RNA (gRNA)[1] appears essential for viral infectivity via, among others, facilitating gRNA strand exchange during reverse transcription (*2, 3*). Our understanding of HIV-1 gRNA dimerization was greatly improved with the identification of a dimerization site located in stem−loop 1 (SL1, nucleotides 243−277 in Figure 1) (*4, 5*). However, studies in viruses produced by tissue culture cells or peripheral blood mononuclear cells indicated that SL1 was not essential for gRNA dimerization. Depending on the studies, it was shown to control from <10 (*1, 6–9*) to 50% (*4, 5, 10–12*) of the gRNA dimerization level seen in viruses isolated 48 h post-transfection. Thus, intracellular or intraviral gRNA dimerization is possible without a functional SL1. This shows that one or more SL1-independent dimerization sites exist in HIV-1 gRNA. These sites are generally believed to be located well within the 5′ first 1000 nucleotides (nt) of gRNA, because nt 1−500 of HIV-1 gRNA appear to be sufficient for full gRNA dimerization (*13*). What is unclear is their precise molecular location.

We focused on the 5′ untranslated region (5′ UTR) of gRNA, because in vitro interaction studies (*14*) as well as electron microscopic (*15*) evidence suggest the existence of a dimerization site, called the 5′ dimer linkage sequence (5′ DLS) (*14*), within the R region. [The R region (nt 1−97) encodes two stem−loop structures (Figure 1).] This was further stimulated by recent in vitro evidence suggesting that a key element of the 5′ DLS is the GGGAGCUCUC40 palindrome located near the tip of the 5′ TAR stem−loop (Figure 1) (*16*). However, these tentative results have their limitations. (1) The two in vitro interaction studies (*14, 16*) involved short HIV-1 RNA transcripts; such partial transcripts can suffer from artifactual folding (*37*). (2) The electron microscopic evidence (*15*) was low-resolution (±50 nt) and based on the study of gRNA dissolved in a partially denaturing buffer containing 2.5 M urea and 50% formamide; moreover, the electron microscopic study implicated the R-U5 hairpin (Figure 1) rather than the TAR stem−loop. Here, we studied the full-length genome isolated from virions, and we studied it under nondenaturing buffer conditions. To make our survey sufficiently exhaustive, only 6 nt were left unmutated in the 5′ UTR, if the results of Shen et al. (*11*) are also considered. In addition, several nucleotides immediately downstream of the 5′ UTR were mutated and investigated.

† This work was supported by CIHR Grant 12312 and MRC Group Grant 13918 to M.L.

* To whom correspondence should be addressed: Room 108, Lady Davis Institute for Medical Research, Jewish General Hospital, 3755 Cote Ste Catherine, Montreal, Quebec, Canada H3T 1E2. E-mail: mi.laughrea@mcgill.ca. Telephone: (514) 340-8260, ext. 5273. Fax: (514) 340-7502.

[1] Abbreviations: DIS, dimerization initiation site; DLS, dimer linkage sequence; Gag, group specific antigen; gRNA, genomic RNA; HIV-1, human immunodeficiency virus type 1; klh, kissing-loop hairpin; nt, nucleotide; PBMC, peripheral blood mononuclear cell; PBS, primer binding site; Pr55 gag, Gag polyprotein; SD, splice donor; SIV, simian immunodeficiency virus; SL, stem−loop; TAR, transactivation response element; UTR, untranslated region; WT, wild-type.

10.1021/bi7023173 CCC: $40.75
Published on Web 02/16/2008

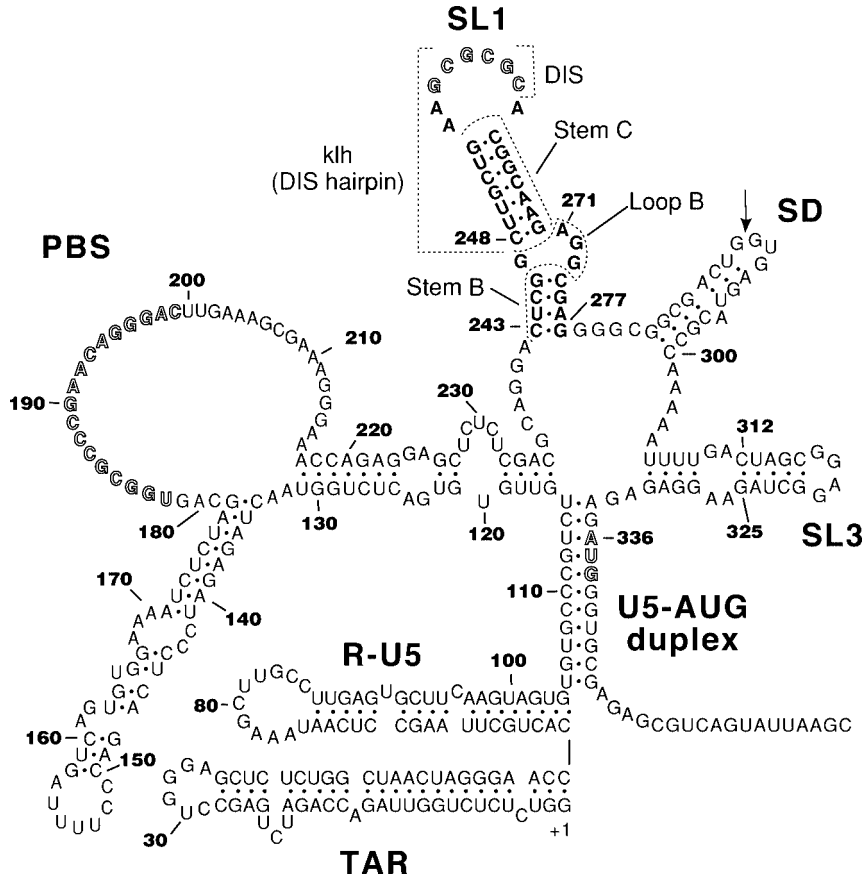

FIGURE 1: Postulated stem–loop diagram of the 5′ untranslated region of HIV-1_{HXB2} genomic RNA. The primer (tRNAlys3) binding site (PBS), the dimerization initiation site (DIS), and the AUG initiation codon of the *gag* gene are highlighted, and the cleavage site within the 5′ major splice donor (SD) is indicated with an arrow. Earlier evidence for this model and attributions related to this model have been described previously (*1*). The top part of SL1 is called kissing-loop hairpin (klh).

Phylogenetic analysis of base pair covariations strongly suggests that, at some point in the viral life cycle, a sequence of the U5 region (nt 98−181 in Figure 1) base pairs with a sequence surrounding the AUG initiation codon of the Pr55 gag polyprotein, to form an 11 bp duplex in all HIV-1 strains (nt 105−115 and 334−344 in Figure 1) and a 10−13 bp duplex among most other primate lentiviruses, such as HIV-2, SIVcpz, SIVagm, SIVsm, SIVsyk, and SIVmnd (*17, 18*). In each virus, the base pairing, but not the actual nt sequence, was conserved, strongly suggesting that the proposed long-distance interaction is functionally important. Biochemical structure probing supports the existence of this long-distance interaction in mutationally stabilized, but not wild-type, partial HIV-1 RNA transcripts (*17*). In vitro evidence for a role of this interaction in the dimerization of partial HIV-1 transcripts is similarly tentative. On the one hand, stabilization of the putative 11 bp duplex, via mutation of most of its G-U base pairs into G-C or A-U base pairs, stimulated dimerization of partial HIV-1 transcripts (suggesting that artificial duplex formation promotes RNA dimerization); on the other hand, destabilization of the putative wild-type duplex did not reduce the level of dimerization (suggesting that the duplex, if it exists in the wild type, has no impact on dimerization) (*17*). In sum, it is not known if this U5-AUG sequence plays a role as a duplex in the dimerization of wild-type HIV-1 partial transcripts, let alone HIV-1 gRNA, but it is tempting to speculate that it might.

In this paper, evidence of a second HIV-1 gRNA dimerization site located in the 5′ TAR stem−loop, and of a positive role of the wild-type U5-AUG sequence in gRNA dimerization, as a molecular duplex, is presented. If the U5-AUG sequence base pairs intermolecularly, it would represent a third dimerization site. Otherwise, its stimulatory role would be indirect.

MATERIALS AND METHODS

Plasmid Construction. Plasmid pSVC21.BH10, also called BH10, encodes an infectious HIV-1_{HXB2} molecular clone derived from the IIIB strain of HIV-1 (*4*). The nucleotide positions are based on the nucleotide sequence of HIV-1_{HXB2} gRNA. Mutant plasmids were constructed from pSVC21.BH10 by PCR mutagenesis, with primers listed in Table 1. To prepare those mutants, a DNA fragment extending from *Hpa*I to *Spe*I was synthesized with sequences at proper sites mutated by PCR and ligated into pSVC21.BH10. To prepare double or multiple mutations in one plasmid, one mutation was first introduced into pSVC21.BH10, another mutation was introduced into the mutated pSVC21.BH10, etc. After mutagenesis with PCR and ligation, the inserted fragments were sequenced (ACGT Inc., Toronto, ON), to verify that the intended mutation, and no other mutation, was introduced.

Cell Cultures and Transfections. 293T, HeLa, or Cos-7 cells were cultured at 37 °C in a culture medium consisting of Dulbecco's modified Eagle's medium (DMEM), 10% fetal calf serum, ampicillin, and streptomycin (Invitrogen). Cells were transfected with the plasmids described above using the Lipofectamine 2000 method (Invitrogen) and cultured

Table 1: Primers Used To Construct Most Mutants in This Paper

mutation	effect on RNA sequence	sense primer(s)[a]
ΔTAR	nt 1−57 deleted	cagctgctttttgcctgtactg cactgcttaagcctcaataaagc
Δ16	nt 16 deleted	ctgggtctctctggttag ccagatctgagcctgggag
A34U	A34 replaced with U	ccagatctgagcctgggTgctctctggctaactagg
U37A	U37 replaced with A	cagatctgagcctgggagcActctggctaactagggaac
M34M37	A34U + U37A	ccagatctgagcctgggTgcActctggctaactagggaac
ΔR-U5	nt 58−104 deleted	ctctggctaactagggaacc tgtgcccgtctgttgtgtgac
Δ99–123	nt 99−123 deleted	gcttgccttgagtgcttcaa actctggtaactagagatcc
ΔCCC	CCC111 deleted	gtgcttcaagtagtgtgtg gtctgttgtgtgactctgg
M105	see Table 3	ccttgagtgcttcaagtagtgGgtTccTAtGAgttgtgtgactctggtaactag
M105-1	see Table 3	ccttgagtgcttcaagtagtgAgtAccTAtctgttgtgtgactctggtaactag
M105-2	see Table 3	ccttgagtgcttcaagtagtgGgtTccTAtAGgttgtgtgactctggtaactag
M105-3	see Table 3	ccttgagtgcttcaagtagtgGCtTGccAtAGgttgtgtgactctggtaactag
ΔPBSh	nt 117−235 deleted	gcttcaagtagtgtgtgcccgtctg cgcaggactcggcttgctgaagcgc
Δ125–156	nt 125−156 deleted	gtgtgcccgtctgttgtgtgac agtcagtgtggaaaatctc
Δ158–182	nt 158−182 deleted	gagatccctcagacccttta ggcgcccgaacagggacttg
Δ153–171	nt 153−171 deleted	gtaactagagatccctcagaccc tctctagcagtggcgcccgaac
Δ180–215	nt 180−215 deleted	gtgtggaaaatctctagcag ttgaaagcgaaagggaaacc
Δ182–199	nt 182−199 deleted	gtcagtgtggaaaatctctagc aaccagaggagctctctcgac
Δ187–206	nt 187−206 deleted	ggaaaatctctagcagtggcg cgaaagggaaaccagaggag
Δ200–226	nt 200−226 deleted	gcagtggcgcccgaacagggac ctctctcgacgcaggactcgg
Δ203–215	nt 203−215 deleted	gtggcgcccgaacagggacttg aaccagaggagctctctcgac
Δ224–233	nt 224−233 deleted	gcgaaagggaaaccagag gacgcaggactcggcttgc
Δ236–242	nt 236−242 deleted	ccagaggagctctctcga ctcggcttgctgaagcgc
YΔ224–226	nt 224−226 and 248−256 deleted, U200 replaced with C	(1) ctctcgacgcaggactcgg gcgcgcacggcaagag (2) cgaaagggaaaccagag ctctctcgacgcaggactc (3) gcgcccgaacagggacCtgaaagcgaaagggaaac
ΔDIS	GCGCGC262 deleted	ctcgacgcaggactcggcttgctgaa acggcaagaggcgagg
ΔTARΔDIS	GCGCGC262 and nt 1−57 deleted	(1) cagctgctttttgcctgtactg cactgcttaagcctcaataaagc (2) ctcgacgcaggactcggcttgctgaa acggcaagaggcgagg
C258G	C258 replaced with G	gcaggactcggcttgctgaagGgcgcacggcaagaggcg
C258GΔ99–123	C258 replaced with G and nt 99−123 deleted	(1) gcaggactcggcttgctgaagGgcgcacggcaagaggcg (2) gcttgccttgagtgcttcaa actctggtaactagagatcc
C258GΔ102−108Δ116–123	C258 replaced with G and nt 102−108 and 116−123 deleted	(1) gcaggactcggcttgctgaagGgcgcacggcaagaggcg (2) gccttgagtgcttcaagta cccgtct actctggtaactagagatcc
C258GΔPBSh	C258 replaced with G and nt 117−235 deleted	(1) gcttcaagtagtgtgtgcccgtctg cgcaggactcggcttgctgaagcgc (2) gcaggactcggcttgctgaagGgcgcacggcaagaggcg
R2Δ224–226	C258 replaced with G, nt 224−226 deleted, and U200 replaced with C	(1) gcaggactcggcttgctgaagGgcgcacggcaagaggcg (2) cgaaagggaaaccagag ctctctcgacgcaggactc (3) gcgcccgaacagggacCtgaaagcgaaagggaaac
ΔSD	nt 312−325 deleted	gcacggcaagaggcgaggggc tggtg aaaaattttgactagcggaggc
M334	see Table 3	gcggaggctagaaggagagTCatgggAgcCagagcgtcagtattaagcgg
M334-1	see Table 3	gcggaggctagaaggagagagatgggtgcTagagcgtcagtattaagcgg
M334-2	see Table 3	gcggaggctagaaggagagCTatgggAgcCagagcgtcagtattaagcgg

[a] The indicated primers are the forward primers used to introduce the mutations into the BH10 plasmid. Deletions are denoted with spaces in the primers, and substitutions are denoted with capital letters.

in 100 mm × 20 mm Petri dishes containing 12 mL of culture medium.

Virus Purification and Isolation of HIV-1 Viral RNA. Virus-containing supernatants were collected and centrifuged at 35000 rpm (SW41 rotor, 4 °C, 1 h), through a 2 mL 20% sucrose cushion in phosphate-buffered saline. The virus pellet was dissolved in 400 μL of sterile lysis buffer [50 mM Tris (pH 7.4), 50 mM NaCl, 10 mM EDTA, 1% (w/v) SDS, 50 μg of tRNA/mL, and 100 μg of proteinase K/mL]. Virus samples were incubated at 37 °C for 30 min and then extracted twice at 4 °C with an equal volume of a buffer-saturated phenol/chloroform/isoamyl alcohol mixture (25:24:1 by volume) (Invitrogen), as described previously (*12, 20*). The aqueous phase, containing the viral RNA, was precipitated overnight at −80 °C with 0.1 volume of 3 M sodium acetate (pH 5.2) and 2.5 volumes of 95% (v/v) ethanol and centrifuged at 14000 rpm in an Eppendorf 5145 microcentrifuge at 4 °C for 30 min. The gRNA pellet was rinsed with 70% (v/v) ethanol and dissolved in 10 μL of buffer S [10 mM Tris (pH 7.5), 100 mM NaCl, 10 mM EDTA, and 1% SDS] (*1*).

Electrophoretic Analysis of HIV-1 gRNA. Dimerization of viral RNA was assessed by nondenaturing Northern (RNA) blot analysis as described previously (*12*). Electrophoretic conditions were 4 V/cm for 4 h on a 1% (w/v) agarose (Bioshop Canada) gel in TBE_2 [89 mM Tris, 89 mM borate, and 2 mM EDTA (pH 8.3)] at 4 °C. After electrophoresis, the gel was heated at 65 °C for 30 min in 10% (v/v) formaldehyde, and the embedded RNAs were diffusion transferred to a Hybond N+ nylon membrane (Amersham). After the sample was dried at 37 °C for 1 h, cross-linked (in a UV Stratalinker 2400), and prehybridized at 42 °C for 3 h in 6× SSPE [1× SSPE is 0.15 M NaCl, 10 mM NaH_2PO_4, and 1 mM EDTA (pH 7.4)], 50% (v/v) deionized formamide, 10% (w/v) dextran sulfate, 1.5% SDS, 5× Denhardt's reagent, and 100 μg/mL salmon sperm DNA, the nylon membrane was hybridized overnight in prehybridization buffer devoid of Denhardt's reagent in a rotating hybridization oven at 42 °C to approximately 25 μCi of ^{35}S-labeled antisense RNA 636-296 prepared with the SP6 Megascript kit (Ambion). This was followed by three washes for 40 min at (i) room temperature, (ii) 37 °C, and (iii) 45 °C as described previously (*4*), and exposure to Kodak BioMax MR X-ray film. The ^{35}S label, introduced into the RNA probe via cytidine 5′-(α-thio)triphosphate, optimizes the resolution

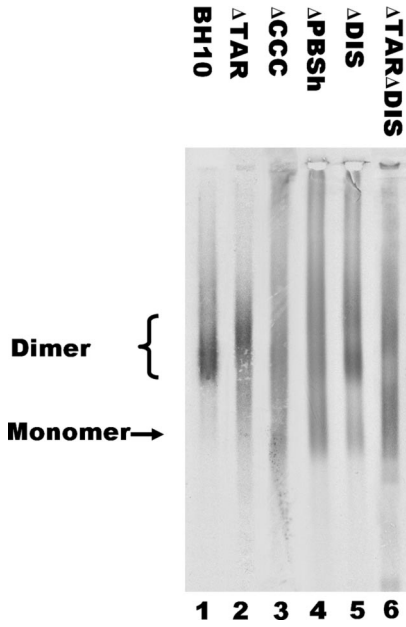

FIGURE 2: Dimerization level and electrophoretic mobility of viral RNA isolated from BH10 (WT), ΔTAR (nt 1−57 deleted), ΔCCC (CCC111 deleted), ΔPBSh (nt 117−235 deleted), ΔDIS (GCGCGC262 deleted), and ΔTARΔDIS virions produced by 293T cells. Genomic RNAs extracted from purified virions were electrophoresed on a nondenaturing 1% (w/v) agarose gel and analyzed by Northern blotting (Materials and Methods). The representative lanes contain viral gRNA isolated from two Petri dishes except BH10 from one, and the exposure time is ~40 min, except that ΔTAR and ΔTARΔDIS were exposed for 25 h. Dimerization level is independent of the amount of gRNA electrophoresed or of the concentration of DNA used in transfections (25-fold range of BH10 and C258G gRNA/proviral DNA concentrations tested) (not shown). It is also known that highly reduced HIV-1 gRNA packaging need not impair gRNA dimerization (*12*).

of the autoradiograms, relative to a ^{32}P label, because ^{35}S is absorbed within 0.3 mm versus 8 mm for ^{32}P.

Densitometric Analysis. The autoradiographs were scanned and analyzed with NIH 1.6.3 Image. Care was taken to scan variously exposed films to guard against overexposed or underexposed bands. Material located near the top of the lanes (e.g., Figure 3A, lanes 2, 8, and 9; Figure 3B, lane 3; and Figure 4A, lane 4) was not taken into account, but the low-mobility gRNA band or shoulder often seen just above the main dimer band was counted as dimer, as in our previous paper (*1*). This method differs from our earlier quantitations (*10–12*): it increases somewhat the percentage dimerization reported in mutants that were less dimeric than WT but does not significantly affect the percentage dimerization reported for WT or mutants that were as dimeric as WT. Low-mobility dimers appear as a separate gRNA band in a number of gel lanes (e.g., Figure 2, lane 5; Figure 3A, lanes 7, 10, and 11; and Figure 4A, lane 15). The low-mobility dimer band or shoulder is usually more prominent in mutants than in WT; otherwise, it is equally prominent. If these low-mobility gRNAs were not considered dimers, the poorly dimeric mutants would be classified as even less dimeric, and this would reinforce the conclusions of this paper. The diffuse character of many bands may reflect conformational diversity among the gRNA molecules. It is not due to poor resolution of the gels because heat-denatured gRNAs formed a sharp band at the monomer position (Figure 7). The RNA bands seen here are not more diffuse, and sometimes sharper, than

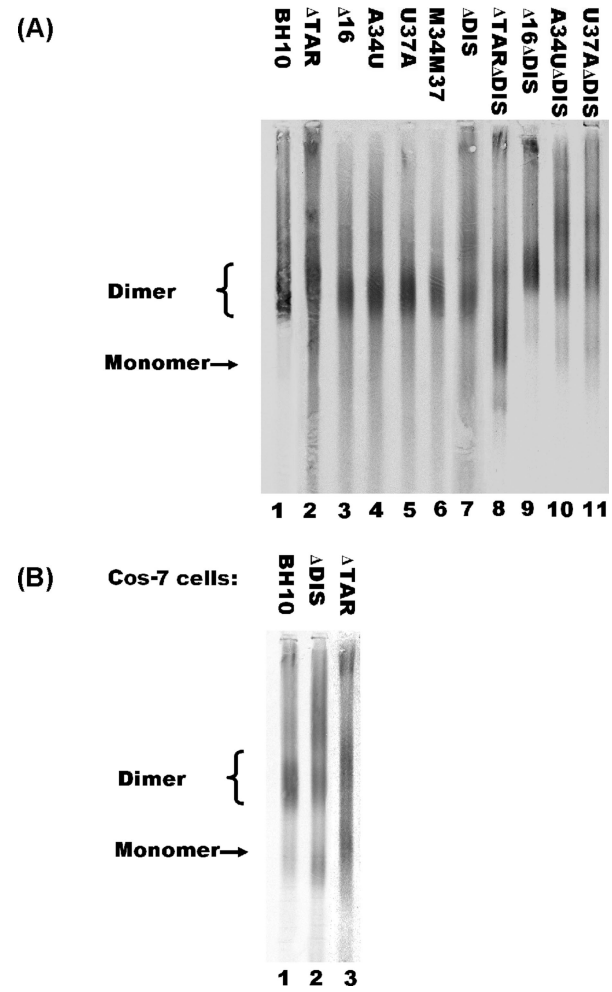

FIGURE 3: Electrophoretic mobility and dimerization level of viral RNA isolated from WT and virions with mutations in 5′ TAR or SL1 elements or both. Genomic RNA was analyzed as described in the legend of Figure 2. (A) Genomic RNA isolated from viruses produced by 293T cells. In Δ16, A16 was deleted. In A34U and U37A, A34 and U37 were replaced with U and A, respectively. (B) WT, ΔTAR, and ΔDIS gRNA isolated from virions produced by Cos-7 cells.

what was seen in earlier studies (*4, 5, 7, 8, 10, 13*). In an effort to optimize the RNA preparation and the electrophoretic conditions, it was found that BH10 and ΔDIS gRNA bands did not become less heterogeneous as a result of (a) doubling or halving the ionic strength of the virus lysis buffer, (b) doubling or halving the ionic strength of buffer S, and (c) reducing or increasing the electrophoretic voltage by 50% (unpublished data).

RESULTS

The search for gRNA dimerization sites other than SL1 in the 5′ UTR is hindered by the presence of SL1 near the middle of the 5′ UTR (Figure 1). On the one hand, mutations may indirectly inhibit gRNA dimerization via obstructing SL1 folding or function. For example, inactivating SL3 (Figure 1), via deletion of its 5′ strand and apical loop, inhibited gRNA dimerization, but SL3 inactivation and DIS inactivation were no more inhibitory than DIS inactivation, suggesting that SL3 played no direct, or SL1-independent, role in gRNA dimerization (*11*). This idea was strengthened by showing that deletion of SL3 had a minimal impact on

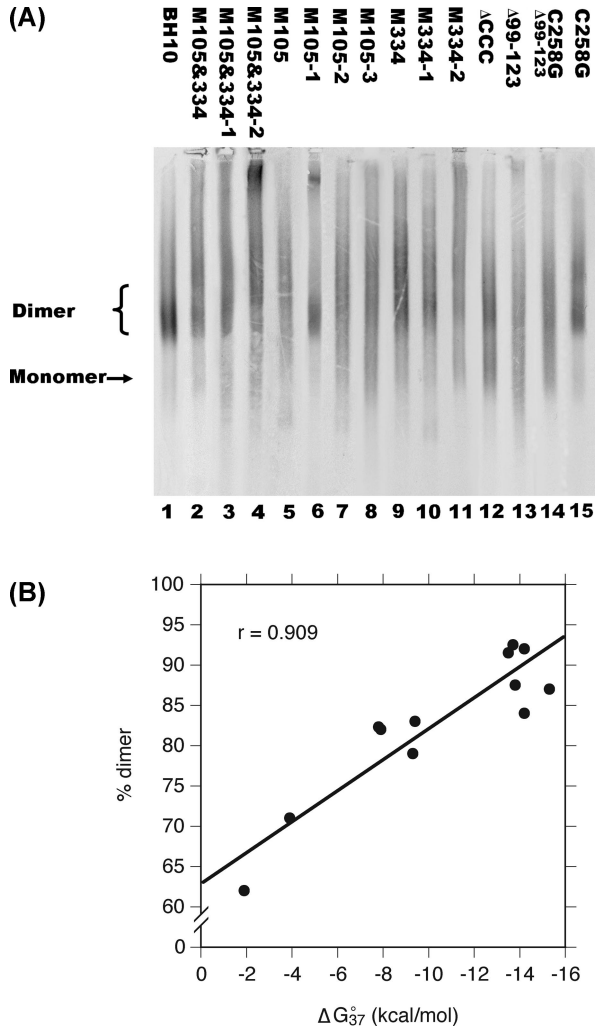

FIGURE 4: (A) Dimerization level and electrophretic mobility of viral RNA isolated from WT and virions bearing mutations in the U5-AUG duplex, the DIS, or both. All virions were produced by 293T cells. See Table 4 for definitions of most mutants. In C258G, C258 was replaced with G. (B) Plot of ΔG°_{37} and % dimer data listed in Table 4. The plot shows a correlation between the gRNA dimerization level of the U5-AUG duplex mutants and the calculated stability of the putative duplexes.

gRNA dimerization (*11*). [The dimerization initiation site (DIS; Figure 1) is a palindromic hexanucleotide located in the apical loop of SL1.] On the other hand, inactivating dimerization sites other than SL1 might have an impact that is concealed by SL1. For example, in vitro RNA interaction studies showed that the impacts of inactivating the 5′ DLS or the 3′ DLS (nt 296–401) were concealed when the RNA transcripts included SL1 (*14, 16, 19*−*22*). In this report, selected mutations were studied in the context of a disabled SL1, to detect effects concealed in the presence of a normal SL1, and to verify whether an inhibitory effect was not entirely due to an influence on SL1 folding or function.

Intriguing Mutants. 293T cells were transfected in parallel with equal amounts of pSVC21.BH10 or mutant plasmids, unless stated otherwise. After 48 h, viruses were isolated, and their genomic RNA was extracted and analyzed by nondenaturing agarose gel electrophoresis, Northern blotting, and autoradiography (Materials and Methods).

Figure 2 and Table 2 present gRNAs from the wild-type (WT) BH10 and intriguing mutants such as ΔTAR (Δ1–57; see Figure 1), ΔCCC (Δ109–111), ΔPBSh (Δ117–235), ΔDIS (Δ257–262), and ΔTARΔDIS (Δ1–57 and Δ257–262). Δ means "deletion of", and the numbers refer to the first and last deleted nucleotide. ΔTAR or ΔDIS had no or little influence on the percentage of gRNA dimers (compare lane 1 to lanes 2 and 5 in Figure 2). However, ΔTARΔDIS yielded a highly synergistic 50% reduction, on average, of the percentage of dimerization (Figure 2, lane 6; Table 2). The level of genomic RNA dimerization was also significantly reduced, to 67 and 75% of that of WT, respectively (Table 2), when CCC111 or the PBS stem−loop was deleted (compare lane 1 to lanes 3 and 4 in Figure 2). ΔTAR, ΔPBSh, ΔDIS, and ΔTARΔDIS decreased gRNA dimer mobility or increased the proportion of low-mobility dimers (Figure 2 and Table 2), indicating that gRNA dimer conformation in those mutants may be more extended than that in WT.

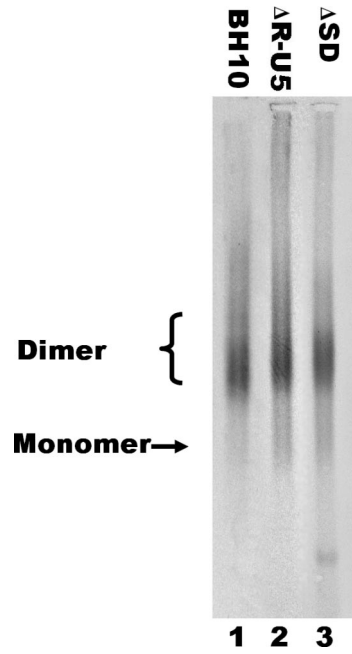

FIGURE 5: Dimerization level and electrophoretic mobility of viral RNA isolated from WT, ΔR-U5, and ΔSD virions produced by 293T cells. In ΔR-U5 and ΔSD, nt 58−104 and 282−300 were deleted, respectively.

Role of the 5′ TAR Stem−*Loop in gRNA Dimerization.* Figure 3A shows that point mutations in or near the 5′ TAR palindrome did not affect the dimeric RNA conformation or the dimerization level (lanes 1–4). Mutations A34U and U37A weaken the GGGAGCUCUC40 palindrome of the 5′ TAR stem−loop; Δ16 allows formation of an uninterrupted 16 bp stem (nt 5−21 and 39−54) that probably hinders facile exposure of the 5′ TAR palindrome (*16*). To verify if putative effects of these mutations were more easily detectable in the absence of an active DIS, the double mutants Δ16ΔDIS, A34UΔDIS, and U37AΔDIS were prepared. The results show that all three mutations reduced the electrophoretic mobility of dimeric RNA by 10% (compare lanes 9–11 to lane 7 in Figure 3A) without, however, reducing the percentage of dimerization (Figure 3A, lanes 9–11).

In HIV-1 produced by Cos-7 cells, gRNA dimerization appears to be more easily inhibited by mutations in the DIS or the viral protease (*10–12*) than in HIV-1 produced by 293T cells (*1*), and the WT dimerization level appears to be slightly

Table 2: Impact of 5′ UTR Mutations, Exclusive of Some U5-AUG Duplex Mutations, on the Percentage of gRNA Dimerization and Dimer Mobility in Viruses Produced by 293T Cells

virus[a]	% dimerization (±SE)[b]	mutant/WT[c]	inhibitory effect[d]	mobility of main dimer band(s) (% of WT mobility)
BH10 (WT)	92 ± 0.9	100	−	100
ΔTAR	88 ± 2.4	96 ± 2.8	−	85–90
ΔCCC	62 ± 1.1	67 ± 1.4	+++	100
ΔPBSh	69 ± 1.2	75 ± 1.5	++	75–100
ΔDIS	88 ± 1.6	96 ± 2.0	−	100; 70–75
ΔTARΔDIS	46 ± 2.3	50 ± 2.6	+++	85–90
Δ16	87 ± 2.1	95 ± 2.5	−	100
A34U	90 ± 1.4	98 ± 1.8	−	100
U37A	87 ± 2.1	95 ± 2.5	−	100
M34M37	85 ± 2.2	92 ± 2.6	−/+	100
Δ16ΔDIS	90 ± 0.6	98 ± 1.2	−	85–90
A34UΔDIS	88 ± 1.7	96 ± 2.1	−	85–90; 55–60
U37AΔDIS	89 ± 1.2	97 ± 1.6	−	85–90; 55–60
C258G	91 ± 1.2	99 ± 1.6	−	100; 70–75
ΔDIS	88 ± 1.6	96 ± 2.0	−	100; 70–75
ΔPBSh	69 ± 1.2	75 ± 1.5	++	75–100
C258GΔPBSh	66 ± 2.2	72 ± 2.5	++	75–100
Δ125–156	89 ± 3.5	97 ± 3.9	−	100
Δ153–171	91 ± 1.0	99 ± 1.5	−	100
Δ158–182	90 ± 2.9	98 ± 3.3	−	100
Δ182–199	80 ± 3.2	87 ± 3.6	+	100
Δ187–206	90 ± 3.5	98 ± 3.9	−	100
Δ180–215	89 ± 1.0	97 ± 1.4	−	100
Δ203–215	88 ± 2.5	96 ± 2.9	−	100
Δ200–226	84 ± 4.0	92 ± 4.5	−/+	75–100
Δ224–233	79 ± 2.0	86 ± 2.3	+	75–100
R2Δ224–226[e]	80 ± 1.5	87 ± 1.8	+	100; 70–75
YΔ224–226[f]	80 ± 0.5	87 ± 1.0	+	100; 70–75
Δ236–242	78 ± 5.2	85 ± 5.7	+	75–100
ΔCCC	62 ± 1.1	67 ± 1.4	+++	100
Δ99–123	69 ± 2.0	75 ± 2.3	++	75–100
C258GΔ99–123	68 ± 3.0	74 ± 3.3	++	75–100
M105&334-2	93 ± 2.3	101 ± 2.7	−	75–100
M105-2	82 ± 3.0	90 ± 3.4	+	75–100
M334-2	79 ± 1.8	86 ± 2.1	+	75–100
M105-1	92 ± 1.1	100 ± 1.5	−	100
M105-3	71 ± 4.4	77 ± 4.8	++	75–100
ΔSD	88 ± 1.6	96 ± 2.0	−	100
ΔR-U5	86 ± 1.5	93 ± 1.9	−/+	100

[a] Mutated nucleotides are defined in Table 1. Results for ΔCCC, ΔPBSh, and ΔDIS are repeated once to ease comparisons and coordination with figures. [b] Percentage of dimeric gRNA relative to the amount of dimer and monomer gRNA determined by native Northern blotting. The standard error of three to five independent experiments (independent virus preparations) is indicated. [c] Dimerization level of mutant viruses relative to that of WT, multiplied by 100. [d] Effect seen in grown-up virions. −, ≥95% of that of WT; −/+, 90–95% of that of WT; +, 80–90% of that of WT; ++, 70–80% of that of WT; +++, <70% of that of WT. [e] R2Δ224–226 includes C258G, U200C, and Δ224–226. [f] YΔ224–226 includes Δ248–256, U200C, and Δ224–226.

Table 3: Impact on gRNA Dimerization of Mutations in Viruses Produced by Cos-7 or HeLa Cells

	Cos-7[b]		HeLa	
virus[a]	% dimerization (±SE)	mutant/WT	% dimerization (±SE)	mutant/WT
BH10 (WT)	84 ± 1.0	100	72 ± 1.7	100
ΔTAR	46 ± 4.6	55 ± 5.5	33	46
ΔCCC	−	−	36 ± 1.4	50 ± 2.3
ΔDIS	71	85	63 ± 3.0	88 ± 4.7
C258G	61	73	55 ± 4.1	76 ± 5.9
ΔPBSh	58 ± 1.6	69 ± 2.1	39 ± 0.4	53 ± 1.4
C258G	48 ± 2.8[c]	57 ± 3.3	−	−
C258GΔPBSh	47 ± 2.0	56 ± 2.5	−	−
C258GΔ102–108Δ116–123	51 ± 0.5	61 ± 0.9	−	−
ΔPBSh	44 ± 2.5	52 ± 3.0	−	−
Δ158–182	67 ± 2.8	80 ± 3.5	−	−
Δ182–199	63 ± 3.2	74 ± 3.9	−	−
Δ187–206	67 ± 1.8	80 ± 2.4	−	−
Δ180–215	75 ± 2.1	89 ± 2.7	−	−
Δ203–215	78 ± 1.8	93 ± 2.4	−	−
Δ200–226	63 ± 2.5[d]	75 ± 3.1	−	−
Δ224–233	46	55	−	−
Δ236–242	55 ± 2.1[d]	65 ± 2.6	−	−

[a] Mutated nucleotides are defined in Table 1. [b] Results below the blank row are mostly unpublished data of L. Jetté, N. Shen, and M. Laughrea. These data can be quantitatively compared to each other and to the results of Shen et al. (*10, 11*) and Laughrea et al. (*12*), three of which are included to ease comparisons. Low-mobility gRNAs (defined in Densitometric Analysis) were not counted as dimers by Jetté et al.; this explains the lower percent dimerization reported for C258G and ΔPBSh below the blank row. The percent dimerization for BH10 was 84%, as in this paper. [c] From Shen et al. (*10*). [d] From Shen et al. (*11*).

reduced (these impressions require comparison of results from separate papers). The effect of ΔTAR in virions produced by Cos-7 cells was accordingly studied. We found that ΔTAR inhibited gRNA dimerization to ∼55% of the WT level, i.e., more than ΔDIS (Table 3), in addition to reducing dimer and monomer mobility by 10% (Figure 3B). Similar effects on RNA dimerization and mobility were obtained with viruses produced by HeLa cells, except that gRNA was approximately 10% less dimeric than in viruses produced by Cos-7 cells (Table 3).

Genomic RNA Dimerization Correlates with the Base-Pairing Potential of the U5-AUG Sequence. We asked whether a correlation existed between the theoretical stability of the U5-AUG duplex and the gRNA dimerization yield in isolated viruses. Multiple point mutations were introduced into the U5 and/or AUG strands to either destabilize the putative duplex or leave it unchanged in stability despite up to 10 base substitutions per mutant (Table 4). Care was taken not to affect the amino acid sequence of Pr55 gag or create an unfavorable context for AUG codon recognition (*23*). The stability of the duplex was theoretically maintained in mutants M105&334 and M105&334-2 (10 base substitutions for each mutant), M105-1 (four base substitutions in the U5 strand), M334-1, and M105&334-1. The duplex was unstable in mutants M105-3 and ΔCCC (seven-base substitution and 3 nt deletion, respectively, in the U5 strand). The duplex was moderately destabilized in mutants such as M334-2, M105-2, M105, and M334 (four to six base substitutions for each mutant). The gRNA dimerization levels seen in the various U5-AUG mutants are shown in Figure 4A and listed in Table 4.

No or very few gRNA monomers were seen in M105&334, M105&334-1, M105&334-2, and M105-1 (Figure 4A, lanes 2–4 and 6); a considerable proportion of monomers was seen in M105-3 and ΔCCC (Figure 4A, lanes 8 and 12; Table 2), and M105, M105-2, and M334-2 ranked somewhere between those extremes (Figure 4A, lanes 5, 7, and 11; Table 2). Figure 4B shows that there was a good correlation [linear correlation coefficient (r) = 0.91] between the dimerization yield and the Gibbs standard free energy of duplex formation (ΔG°_{37}) of the various putative U5-AUG duplexes. No correlation was seen between gRNA dimerization and the number of nucleotide substitutions per mutant (not shown). This suggests that U5-AUG duplex formation, independent of sequence, stimulates gRNA dimerization in isolated

Table 4: Impact of Mutations in the Putative U5-AUG Duplex on the Calculated Standard Free Energy of Duplex Formation and Observed Genomic RNA Dimerization in Viruses Produced by 293T Cells[a]

Mutant	# modifications	Sequence	ΔG°_{37} (kcal/mol)	%dimers ±SE
WT	0	5′-UGUGCCCGUCU-115 344-GCGUGGGUAGA-5′	-14.2	92±0.9
M105-1	4	AGUACCUAUCU GCGUGGGUAGA	-13.5	92±1.1
M105&334-1	5	AGUACCUAUCU UCGUGGGUAGA	-13.8	88±2.4
M334-1	1	UGUGCCCGUCU UCGUGGGUAGA	-14.2	84±2.2
M105&334-2	10	GGUUCCUAUAG CCGAGGGUAUC	-13.7	93±2.3
M105&334	10	GGUUCCUAUGA CCGAGGGUACU	-15.3	87±3.5
M105-2	6	GGUUCCUAUAG GCGUGGGUAGA	-7.8	82±3.0
M334-2	4	UGUGCCCGUCU CCGAGGGUAUC	-9.3	79±1.8
M334	4	UGUGCCCGUCU CCGAGGGUACU	-9.4	83±1.8
M105	6	GGUUCCUAUGA GCGUGGGUAGA	-7.9	82±3.4
M105-3	7	GCUUGCCAUAG GCGUGGGUAGA	-3.9	71±4.4
ΔCCC	3	UGUG——GUCU GCGUGGUAGA	-1.9	62±1.1

[a] The percent dimer for each mutant sample represents the average from three to five independent experiments (i.e., independent virus preparations) ± the standard error.

viruses (Figure 4B). This strong correlation between U5-AUG duplex base-pairing potential and gRNA dimerization yield is consistent with an in vitro study of short (368 nt) mutationally stabilized partial HIV-1 RNA transcripts (*17*).

Our results indicate that, since blocking U5-AUG duplex formation is more disabling than ΔDIS, it impedes the function of a DIS-independent dimerization site in viruses produced by 293T cells. It may also impede SL1. The inhibition of gRNA dimerization caused by blocking U5-AUG duplex formation (see ΔCCC, M105-3, or Δ99–123 in Table 2 and Figure 4A) was as strong as the impairment created by deleting the PBS stem−loop (see ΔPBSh in Table 2 and Figure 2), as if disabling the U5-AUG duplex or deleting the PBS stem−loop disturbed the same dimerization site(s). Where are these dimerization sites? The feasibility of a location within the U5-AUG duplex, the PBS stem−loop, the R-U5 stem−loop, and the SD stem−loop (Figure 1) is addressed in the three following sections.

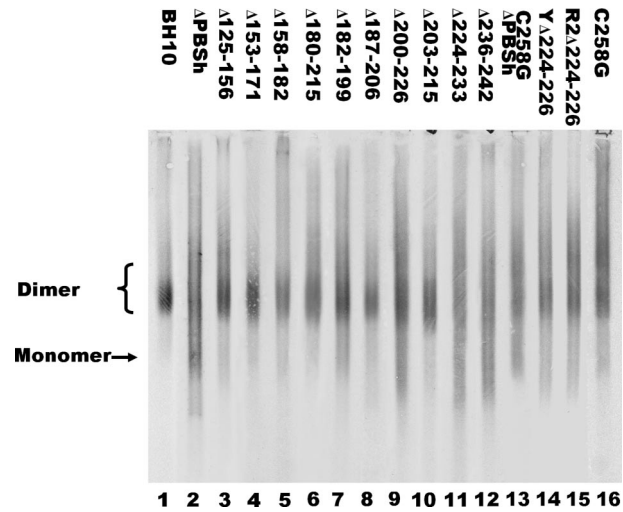

FIGURE 6: Dimerization level and electrophoretic mobility of viral RNA isolated from virions with mutations mostly in the PBS stem−loop. In ΔPBSh, nt 117−235 were deleted. YΔ224–226 consists of Δ248–256, U200C, and Δ224–226. RΔ224–226 consists of C258G, U200C, and Δ224–226. All virions were produced by 293T cells.

The UG-Rich Sequence within and around the U5-AUG Duplex Is Unlikely To Contain a gRNA Dimerization Site. Nucleotides 102–108 and 112–123 flank the central CCC111 segment of the U5-AUG duplex and contain seven UG dinucleotides and two UGUGUG palindromes. Since the nucleocapsid protein binds with remarkable affinity to UG- and GUG-rich oligonucleotides (*24–27*) and stimulates the dimerization of partial HIV-1 RNA transcripts (*28, 29*) and HIV-1 gRNA (*12*), it has been suggested that these regions might play a direct role as a self-complementary dimerization site. Our experiments do not support this possibility. First, M105-1 and M105M334-2 mutated two and three of these UG dinucleotides, respectively, without inhibiting gRNA dimerization. Second, Δ99–123 did not inhibit gRNA dimerization any more than ΔCCC (Table 2 and Figure 4A, lanes 12 and 13). Third, in viruses produced by Cos-7 cells, inactivation of the DIS and deletion of GUGUGUG108 and GUUGUGUG123 did not inhibit gRNA dimerization any more than DIS inactivation (compare C258G to C258GΔ102–108Δ116–123 in Table 3). Our results therefore indicate that nt 100−120 stimulate gRNA dimerization via formation of a U5-AUG duplex, rather than through UGUGUG palindromic interactions.

Deletion of the SD Stem−Loop or the R-U5 Stem−Loop Does Not Affect gRNA Dimerization or Dimer Conformation. Figure 5 and Table 2 show that ΔSD (Δ282–300) or ΔR-U5 (Δ58–104) viruses produced WT-level gRNA dimerization yields and dimer mobilities. This suggests that the SD and R-U5 stem−loop forms (Figure 1) contain no dimerization site and that deleting them does not influence the roles of the 5′ TAR and the DIS in gRNA dimerization. In viruses produced by Cos-7 cells, it had been shown that gRNA dimerization was not affected by deletion of most of the SD stem−loop (*11*) or deletion of the apical loop of the R-U5 stem−loop in the absence or presence of a functional SL1 (*12*).

The PBS Stem−Loop Is Unlikely To Contain a Genomic RNA Dimerization Site. If the PBS stem−loop contains a dimerization site, it should be possible to find a segment

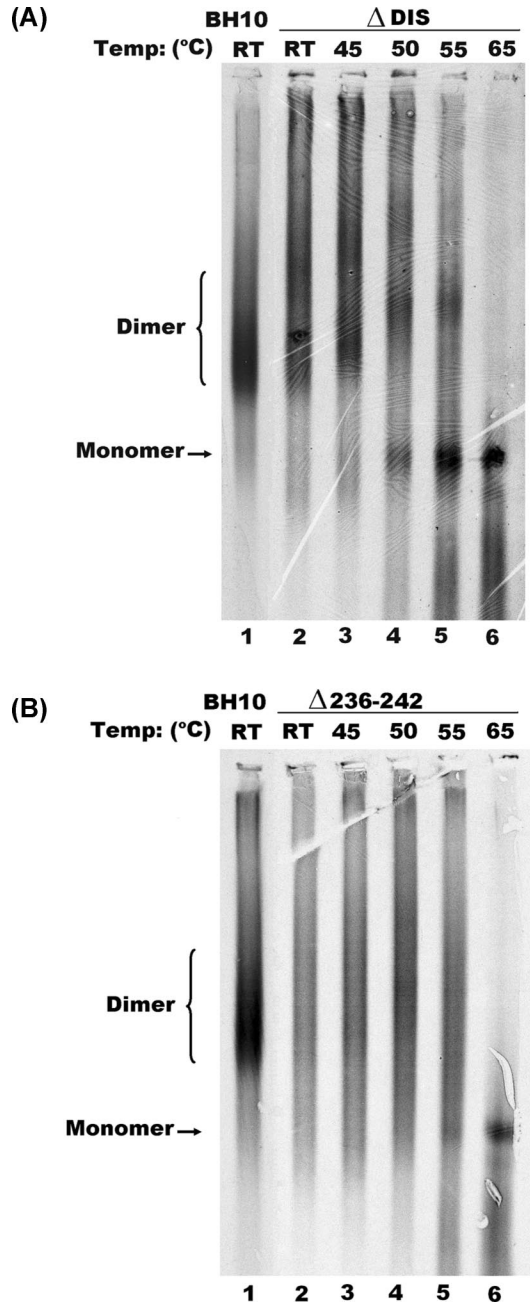

FIGURE 7: Dimerization level and thermal dissociation of gRNA isolated from ΔDIS and Δ236–242 virions produced by 293T cells. Genomic RNA samples were incubated at the indicated temperatures for 10 min in buffer S before electrophoresis and Northern blotting as in Figure 2. (A) Genomic RNA isolated from ΔDIS virions. (B) Genomic RNA isolated from Δ236–242 virions.

within the PBS stem−loop that has as much, or nearly as much, impact on gRNA dimerization as the whole stem−loop. Accordingly, we studied the effect of deleting contiguous portions of the PBS stem−loop.

Together with Table 2, Figure 6 shows that most segments of the PBS stem−loop played no role in gRNA dimerization. Δ125–156, Δ153–171, Δ158–182, Δ180–215, Δ187–206, or Δ203–215 had no or little impact on gRNA dimerization. Thus, the central 75% (i.e., nt 125−215; see Figure 1) of the PBS stem−loop contributed little to the production of dimeric gRNA in grown-up viruses. The results also imply that the central stem (nt 125–131 and 217–223) of the PBS stem−loop is not needed as a duplex for WT-level production of gRNA dimers in grown-up viruses. The inhibitory effect of Δ182–199 should be taken in context: Δ180–215, which includes Δ182–199, did not inhibit gRNA dimerization. Δ180–215 and Δ182–199 fully and partially delete, respectively, the main bulge of the PBS stem−loop (Figure 1). Full deletion of a secondary structure feature is likely to have fewer collateral effects than fractional deletion: Δ182–199 may have exposed nt 180, 181, and 200–215 in a way that made them interact artifactually with other gRNA domains. The marginal inhibitory effect of Δ200–226, together with the inhibitory effect of R2Δ224–226 (C258G, U200C, and Δ224–226), suggests that nt 216–223 played no role in gRNA dimerization either. The 5′ end of the PBS stem−loop (nt 116–124) was not specifically investigated; however, Δ99–123 had no greater impact than the deletion of CCC111 (Table 2) in viruses produced by 293T cells, and C258GΔ102–108 Δ116–123 did not inhibit gRNA dimerization any more than C258G (Table 3) in viruses produced by Cos-7 cells. These results suggest that mutating the 5′ end of the PBS stem−loop had no visible effect on gRNA dimerization.

Interestingly, deletions disabling the 3′ end of the PBS stem−loop (Δ224–233; R2Δ224–226) or the sequence linking the PBS stem−loop to SL1 (Δ236–242) produced half of the inhibitory effect obtained with ΔPBSh (Table 2). Since these mutants are more inhibitory than inactivation of the DIS (Table 2 and Figure 7), they must have hampered more than SL1 with regard to gRNA dimerization. It is difficult to imagine how nt 224–233 or 236–242 could constitute a dimerization site.

Most of the PBS stem−loop mutants were also studied in viruses produced by Cos-7 cells. The results confirmed the importance of the 3′ end of the PBS stem−loop and the smaller role of nucleotides located upstream (Table 3).

DISCUSSION

Synopsis of the Search for Non-TAR and Non-DIS Dimerization Site(s) within the 5′ UTR. Our results show that, in viruses produced by 293T cells, ΔTAR, ΔPBSh, ΔDIS, and C258G changed the gRNA dimer conformation, while ΔTARΔDIS exhibited the lowest gRNA dimerization level, and Δ99–123, ΔCCC, and ΔPBSh exhibited the second lowest level, among all the mutants. ΔTARΔDIS viruses still yielded ~45% dimeric gRNA. Extensive analysis of mutations within the PBS stem−loop uncovered no indication that this region might act as a dimerization site. Deletion of the R-U5 stem−loop (above and ref *12*), the SD stem−loop (above), and SL3 (*11*) had no or little effect on gRNA dimerization, making the presence of a dimerization site in these RNA motifs unlikely. The U5-AUG duplex has either an indirect or a direct stimulatory role in gRNA dimerization, depending on whether the duplex is intra- or intermolecular. In the event, unlikely on simple theoretical grounds, that the duplex is intermolecular, the U5-AUG sequence would become the third dimerization site of the 5′ UTR, after the sites located in the 5′ TAR and in SL1. The gRNA dimerization still seen in ΔTARΔDIS viruses would result from interactions involving sequences downstream from the 5′ UTR, unless an intermolecular U5-AUG duplex could form under these conditions.

Our study of viruses produced by Cos-7 cells is less complete, but the results generally support the conclusions drawn above. Notably, inactivating the DIS and the PBS

stem−loop, or the DIS and the U5-AUG duplex, did not reduce the level of gRNA dimerization more than inactivating the DIS (Table 3). This reinforces the finding that the PBS stem−loop plays no direct role in gRNA dimerization and suggests that the U5-AUG duplex is an intramolecular structure under these conditions.

Overview. Our results can be summarized as follows. (1) The 5′ TAR plays a role in gRNA dimerization, and this role is as important as that of the DIS. This paper provides the first evidence for a role of the 5′ TAR in RNA dimerization in the context of the whole virus [the previous evidence involved a very short RNA studied in vitro (*16*)]. (2) Formation of a U5-AUG duplex stimulates wild-type gRNA dimerization. This paper provides the first experimental evidence for formation of the U5-AUG duplex in wild-type virions (the previous evidence was phylogenetic) and for a role of U5-AUG duplex formation in RNA dimerization in the context of the whole virus [the previous evidence involved a very short and artificially stabilized RNA studied in vitro (*17*)]. (3) The central 75% of the PBS stem−loop contains no gRNA dimerization site and does not generally play any indirect role in the process, despite the significant effect of ΔPBSh on gRNA dimerization. (4) The previously proposed idea that the two UGUGUG palindromes flanking the 5′ strand of the U5-AUG duplex form a dimerization site is not supported. (5) Producing cells can have a quantitative impact on gRNA dimerization. To the best of our knowledge, this is the first demonstration of an effect of producing cells on gRNA dimerization.

Though the relationship between the 5′ TAR stem−loop, or the U5-AUG duplex, and HIV-1 RNA dimerization had been mentioned in two papers (*16, 17*), the evidence was based on the study of partial transcripts, and the U5-AUG duplex could be demonstrated only in stabilized partial transcripts. A historical survey shows that several results obtained with partial HIV-1 transcripts, describing both positive and negative effects of mutations on RNA dimerization, have been contradicted in the context of the whole virus. Most notable are in vitro interaction results: (1) implicating the G-rich sequence GGGGG367, or guanine tetrads, in the dimerization process; (2) showing that loop B of SL1 is dispensable for RNA dimerization; and (3) showing an almost total absence of dimeric RNAs in HIV-1 RNAs that are longer than the 5′ UTR but deprived of the DIS (e.g., refs *4* and *16*). Validation (or refutation) of in vitro interaction studies by work in the context of the whole virus is essential and fundamental because different long-range interactions and secondary and tertiary structures might exist in vivo and differently influence the ability of HIV-1 RNA to form a dimer.

5′ TAR. Five types of evidence indicate that the 5′ TAR contains a gRNA dimerization site. (1) ΔTAR impaired dimerization more than ΔDIS in virions produced by Cos-7 and HeLa cells (Table 3). (2) ΔTAR had effects as large as those of ΔDIS in 293T cells (Figure 2). (3) Mild point mutations in the 5′ TAR palindrome affected gRNA dimer conformation (Figure 3A, lanes 9–11). (4) There is in vitro evidence for loop−loop kissing interactions involving the 5′ TAR (*16*). (5) The structure of the 5′ TAR suggests a dimerization mechanism analogous to the loop−loop kissing interactions proven in SL1; one difference is that the nucleocapsid protein is probably needed to expose the otherwise largely base paired TAR palindrome (*16*). We have recently shown that the proportion of gRNA dimers in ΔDIS virions produced by 293T cells, though 100% of that of WT 48 h after transfection (Table 2) (*1*), was only 40% of that of WT in newly released virions (*1*). Full dimerization of ΔDIS gRNA was achieved over a period of 3−6 h following virion release (*1*). We propose that the 5′ TAR is the main contributor to this intraviral increase in the level of gRNA dimerization. At that moment, the mature nucleocapsid protein is expected to be available in massive numbers (*1, 30*). One prediction of this hypothesis is that ΔTAR gRNA should be much more dimeric than ΔDIS gRNA in newly released virions.

If the 5′ TAR is a dimerization site analogous to SL1, it should be possible to find point mutations in the 5′ TAR palindrome that inhibit gRNA dimerization. This issue remains unresolved because we studied very mild point mutations: A34U and U37A reduce the calculated ΔG°_{37} of TAR palindrome duplex formation from −14.2 to −10.0 kcal/mol and from −14.2 to −11.4 kcal/mol, respectively. Considering that the ΔG°_{37} of DIS duplex formation is −10.4 kcal/mol in subtype B and D virions (where the DIS is GCGCGC) and −7.6 kcal/mol in all other subtypes (where the DIS is GUGCAC), these small reductions might not be enough to visibly impair gRNA dimerization, though they were able to disable in vitro TAR RNA dimerization in the presence of the nucleocapsid protein (*16*).

Since ΔTAR was more inhibitory in viruses produced by Cos-7 and HeLa cells than in viruses produced by 293T cells (Tables 2 and 3; $P < 0.01$), perhaps Δ16, A34U, or U37A would have reduced the percentage of dimeric RNAs in Cos-7 or HeLa cells. It was recently shown that the 5′ TAR plays little or no role in the replication of HIV-1 in SupT1 cells, other than Tat-mediated activation of transcription (*31*). However, their data could not rule out the possibility that specifically inactivating the 5′ TAR could reduce the rate of viral replication up to 5-fold via an impact that is not related to Tat-mediated activation of transcription.

The U5-AUG Sequence Contributes to gRNA Dimerization as a Duplex. We studied a group of mutations in the putative U5-AUG duplex and found a positive role of duplex formation in gRNA dimerization. One implication of this positive role is that spliced RNAs should dimerize less well since they cannot form a U5-AUG duplex. Another implication is that translation could inhibit gRNA dimerization by disrupting the U5-AUG duplex. Our results identify for the first time a role for sequences downstream of the 5′ splice donor site in HIV-1 gRNA dimerization. Previous results had indicated that mutations downstream of the 5′ splice donor, such as around SL3 (*11, 32*), can inhibit gRNA dimerization, without identifying a mechanism.

Extended PBS Stem−Loop. Evidence for a contribution of the extended PBS stem−loop to gRNA dimerization was first provided by showing the effect of deleting nt 200–226 or 236–242 in virions produced by Cos-7 cells (*11*). The extended PBS stem−loop is the PBS stem−loop and the sequence linking it to SL1. Here we present a more detailed investigation that allowed us to shorten to nt 224–242 the size of the extended PBS stem−loop sequence implicated in gRNA dimerization. We propose that mutations within nt 224–242 must have hindered gRNA dimerization by interfering with dimerization sites that include SL1. When

the first 644 nt of BH10 and mutant gRNAs were folded using the algorithm mfold (version 3.2) (*33, 34*), ΔPBSh prevented SL1 formation and Δ224–233 and Δ236–242 moderately inhibited SL1 formation. This supports the idea that ΔPBSh inhibited gRNA dimerization at least via obstruction of the DIS or SL1.

Diverse Minimal Regions Sufficient for WT-like gRNA Dimerization in Grown-up Virions. A recent study, using as a model system gRNAs containing two copies (one authentic and one ectopic) of nt 1–352 (*35*), gave results that are generally in agreement with ours. Our work extends that of Sakuragi et al. (*35*) in at least six ways. (1) It provides evidence based on authentic HIV-1 gRNA. (2) It identifies a role for the 5′ TAR that could not be seen via the choice of mutants made by Sakuragi et al. (*35*). (3) It provides experimental evidence for a mechanism whereby nt 105–115 (or 105–112 in ref *35*) and 334–344 (or 338–352 in ref *35*) promote gRNA dimerization: the formation of a duplex by nt 105–115 and 334–344. (4) It addresses the effects of mutations not only on the proportion of gRNA dimers but also on the conformation(s) of the gRNA dimers. (5) It studies to some extent whether the obtained results are valid in viruses produced by cells other than 293T cells. (6) It investigates the impact of the primer binding site (nt 182–199) on gRNA dimerization in viruses produced by 293T and Cos-7 cells, instead of HeLa cells (*36*). An additional interest of our study is that it can be seen as a convincing test of the validity of the model system championed by Sakuragi et al. (*35*) for the investigation of the mechanism of HIV-1 gRNA dimerization.

Our identification of two seemingly redundant dimerization sites in grown-up virions produced by 293T cells means that, under these conditions, diverse minimal regions sufficient for genome dimerization can be obtained depending on the order in which successive deletions are studied. For example, a different minimal region may have been obtained by Sakuragi et al. (*35*) if their RNA pruning had started with ΔDIS and ended with ΔTAR, instead of starting with ΔTAR, or if their deletion of SL3 had been studied in a less truncated and internally deleted sequence context.

Cell-Type-Dependent Viral RNA Dimerization Level. Wild-type viruses produced by HeLa and Cos-7 cells contained gRNAs that were 20 ± 2 and 8 ± 1.5% less dimeric ($P < 0.01$), respectively, than that of viruses produced by 293T cells (compare Tables 2 and 3). The quantitative effect, relative to WT, of a number of mutations was also cell-dependent. Notably, ΔTAR was more disabling in viruses produced by Cos-7 cells than in viruses produced by 293T cells; ΔCCC, C258G, and ΔPBSh were more disabling in viruses produced by HeLa cells than in viruses produced by 293T cells, and ΔPBSh was more disabling in viruses produced by HeLa cells than in viruses produced by Cos-7 cells ($P < 0.01$ in the five instances; compare mutant/WT ratios in Tables 2 and 3). One implication of these differentials is that cellular factors modulate the exact level of gRNA dimerization. This could be achieved directly, via binding of cellular factors to viral RNAs or proteins, or indirectly via cell-specific differences either in transfection yield (e.g., in proviral DNA copy number per successfully transfected cell) or in proviral DNA transcription yield. If the effective gRNA concentration per transfected cell was larger in 293T cells than in Cos-7 or HeLa cells, a faster rate of viral RNA dimerization, a larger viral RNA dimerization yield, and a smaller apparent impact of mutations may conceivably result, via mass action effects. Interestingly, the percentages of gRNA dimerization seen in young (≤3 h old) WT and ΔDIS viruses produced by 293T cells (*1*) are comparable to the percentages seen in grown-up WT and ΔDIS virions produced by Cos-7 or HeLa cells (Table 3).

In addition, the gRNA profile (nondenaturing Northern blots) of virions produced by 293T cells is similar in all respects (percentage of gRNA dimerization, thermal stability, and heterogeneity of dimer conformation) to the gRNA profile of virions produced by peripheral blood mononuclear cells (PBMCs), which are natural producer cells of HIV-1. This invariance was observed with WT and SL1-defective virions (*8*). It suggests that the properties of HIV-1 viral RNA dimers are similar in virions produced by 293T cells and PBMCs. However, large SL1 deletions impaired viral replication in PBMCs [log(WT/mutant) = 0.8 ± 0.2 (*8*)] 2−3 logarithmic units less than in SupT1 (*8*) or MT4 (*20*) T-cell lines, i.e., to an extent similar to that in point mutations making the DIS nonpalindromic [log(WT/mutant) = 1.45 ± 0.25 (*20*)]. It would be interesting to know the effect of the novel dimerization sequences identified here on HIV-1 replication in PBMCs.

ACKNOWLEDGMENT

We thank Professor Mark A. Wainberg for access to the HIV growth facility.

REFERENCES

1. Song, R., Kafaie, J., Yang, L., and Laughrea, M. (2007) HIV-1 Viral RNA Is Selected in the Form of Monomers that Dimerize in a Three-step Protease-dependent Process; The DIS of Stem-Loop 1 Initiates Viral RNA Dimerization. *J. Mol. Biol. 371*, 1084–1098.
2. Chin, M. P. S., Rhodes, T. D., Chen, J., Fu, W., and Hu, W.-S. (2005) Identification of a major restriction in HIV-1 intersubtype recombination. *Proc. Natl. Acad. Sci. U.S.A. 102*, 9002–9007.
3. Chin, M. P. S., Chen, J., Nikolaitchik, O. A., and Hu, W.-S. (2007) Molecular determinants of HIV-1 intersubtype recombination potential. *Virology 363*, 437–446.
4. Laughrea, M., Jetté, L., Mak, J., Kleiman, L., Liang, C., and Wainberg, M. A. (1997) Mutations in the kissing-loop hairpin of human immunodeficiency virus type 1 reduce viral infectivity as well as genomic RNA packaging and dimerization. *J. Virol. 71*, 3397–3406.
5. Clever, J. L., and Parslow, T. G. (1997) Mutant human immunodeficiency virus type 1 genomes with defects in RNA dimerization or encapsidation. *J. Virol. 71*, 3407–3414.
6. Berkhout, B., and van Wamel, J. L. (1996) Role of the DIS hairpin in replication of human immunodeficiency virus type 1. *J. Virol. 70*, 6723–6732.
7. Sakuragi, J. I., and Panganiban, A. T. (1997) Human immunodeficiency virus type 1 RNA outside the primary encapsidation and dimer linkage region affects RNA dimer stability in vivo. *J. Virol. 71*, 3250–3254.
8. Hill, M. K., Shehu-Xhilaga, M., Campbell, S. M., Poumbourios, P., Crowe, S. M., and Mak, J. (2003) The dimer initiation sequence stem-loop of human immunodeficiency virus type 1 is dispensable for viral replication in peripheral blood mononuclear cells. *J. Virol. 77*, 8329–8335.
9. Moore, M. D., Fu, W., Nikolaitchik, O., Chen, J., Ptak, R. G., and Hu, W.-S. (2007) Dimer initiation signal of human immunodeficiency virus type 1: Its role in partner selection during RNA copackaging and its effects on recombination. *J. Virol. 81*, 4002–4011.
10. Shen, N., Jetté, L., Liang, C., Wainberg, M. A., and Laughrea, M. (2000) Impact of human immunodeficiency virus type 1 RNA dimerization on viral infectivity and of stem-loop B on RNA dimerization and reverse transcription and dissociation of dimerization from packaging. *J. Virol. 74*, 5729–5735.

11. Shen, N., Jetté, L., Wainberg, M. A., and Laughrea, M. (2001) Role of stem B, loop B, and nucleotides next to the primer binding site and the kissing-loop domain in human immunodeficiency virus type 1 replication and genomic-RNA dimerization. *J. Virol. 75*, 10543–10549.
12. Laughrea, M., Shen, N., Jetté, L., Darlix, J. L., Kleiman, L., and Wainberg, M. A. (2001) Role of distal zinc finger of nucleocapsid protein in genomic RNA dimerization of human immunodeficiency virus type 1: No role for the palindrome crowning the R-U5 hairpin. *Virology 281*, 109–116.
13. Sakuragi, J., Ueda, S., Iwamoto, A., and Shioda, T. (2003) Possible role of dimerization in human immunodeficiency virus type 1 genome RNA packaging. *J. Virol. 77*, 4060–4069.
14. Laughrea, M., and Jetté, L. (1996) Kissing-loop model of HIV-1 genome dimerization: HIV-1 RNAs can assume alternative dimeric forms, and all sequences upstream or downstream of hairpin 248–271 are dispensable for dimer formation. *Biochemistry 35*, 1589–1598.
15. Hoglund, S., Ohagen, A., Goncalves, J., Panganiban, A. T., and Gabuzda, D. (1997) Ultrastructure of HIV-1 genomic RNA. *Virology 233*, 271–279.
16. Andersen, E. S., Contera, S. A., Knudsen, B., Damgaard, C. K., Besenbacher, F., and Kjems, J. (2004) Role of the trans-activation response element in dimerization of HIV-1 RNA. *J. Biol. Chem. 279*, 22243–22249.
17. Abbink, T. E., and Berkhout, B. (2003) A novel long distance base-pairing interaction in human immunodeficiency virus type 1 RNA occludes the Gag start codon. *J. Biol. Chem. 278*, 11601–11611.
18. Damgaard, C. K., Andersen, E. S., Knudsen, B., Gorodkin, J., and Kjems, J. (2004) RNA interactions in the 5′ region of the HIV-1 genome. *J. Mol. Biol. 336*, 369–379.
19. Paillart, J. C., Marquet, R., Skripkin, E., Ehresmann, B., and Ehresmann, C. (1994) Mutational analysis of the bipartite dimer linkage structure of human immunodeficiency virus type 1 genomic RNA. *J. Biol. Chem. 269*, 27486–27493.
20. Laughrea, M., Shen, N., Jetté, L., and Wainberg, M. A. (1999) Variant effects of non-native kissing-loop hairpin palindromes on HIV replication and HIV RNA dimerization: Role of stem-loop B in HIV replication and HIV RNA dimerization. *Biochemistry 38*, 226–234.
21. Laughrea, M., and Jetté, L. (1996) HIV-1 genome dimerization: Formation kinetics and thermal stability of dimeric HIV-1Lai RNAs are not improved by the 1–232 and 296–790 regions flanking the kissing-loop domain. *Biochemistry 35*, 9366–9374.
22. Laughrea, M., and Jetté, L. (1997) HIV-1 genome dimerization: Kissing-loop hairpin dictates whether nucleotides downstream of the 5′ splice junction contribute to loose and tight dimerization of human immunodeficiency virus RNA. *Biochemistry 36*, 9501–9508.
23. Kozak, M. (1999) Initiation of translation in prokaryotes and eukaryotes. *Gene 234*, 187–208.
24. Berglund, J. A., Charpentier, B., and Rosbash, M. (1997) A high affinity binding site for the HIV-1 nucleocapsid protein. *Nucleic Acids Res. 25*, 1042–1049.
25. Fisher, R. J., Rein, A., Fivash, M., Urbaneja, M. A., Casas-Finet, J. R., Medaglia, M., and Henderson, L. E. (1998) Sequence-specific binding of human immunodeficiency virus type 1 nucleocapsid protein to short oligonucleotides. *J. Virol. 72* 1902–1909.
26. Vuilleumier, C., Bombarda, E., Morellet, N., Gérard, D., Roques, B. P., and Mély, Y. (1999) Nucleic acid sequence discrimination by the HIV-1 nucleocapsid protein NCp7: A fluorescence study. *Biochemistry 38*, 16816–16825.
27. Paoletti, A. C., Shubsda, M. F., Hudson, B. S., and Borer, P. N. (2002) Affinities of the nucleocapsid protein for variants of SL3 RNA in HIV-1. *Biochemistry 41*, 15423–15428.
28. Morellet, N., De Rocquigny, H., Mély, Y., Jullian, N., Déméné, H., Ottmann, M., Gérard, D., Darlix, J. L., Fournie-Zaluski, M. C., and Roques, B. P. (1994) Conformational behaviour of the active and inactive forms of the nucleocapsid NCp7 of HIV-1 studied by ^{1}H NMR. *J. Mol. Biol. 235*, 287–301.
29. Muriaux, D., De Rocquigny, H., Roques, B. P., and Paoletti, J. (1996) NCp7 activates HIV-1Lai RNA dimerization by converting a transient loop-loop complex into a stable dimer. *J. Biol. Chem. 271*, 33686–33692.
30. Kaplan, A. H., Manchester, M., and Swanstrom, R. (1994) The activity of the protease of human immunodeficiency virus type 1 is initiated at the membrane of infected cells before the release of viral proteins and is required for release to occur with maximum efficiency. *J. Virol. 68*, 6782–6786.
31. Das, A. T., Harwig, A., Vrolijk, M. M., and Berkhout, B. (2007) The TAR hairpin of human immunodeficiency virus type 1 can be deleted when not required for Tat-mediated activation of transcription. *J. Virol. 81*, 7742–7748.
32. Russell, R. S., Hu, J., Bériault, V., Mouland, A. J., Laughrea, M., Kleiman, L., Wainberg, M. A., and Liang, C. (2003) Sequences downstream of the 5′ splice donor site are required for both packaging and dimerization of human immunodeficiency virus type 1 RNA. *J. Virol. 77*, 84–96, 3891.
33. Mathews, D. H., Sabina, J., Zuker, M., and Turner, D. H. (1999) Expanded sequence dependence of thermodynamic parameters improves prediction of RNA secondary structure. *J. Mol. Biol. 288*, 911–940.
34. Zuker, M. (2003) Mfold web server for nucleic acid folding and hybridization prediction. *Nucleic Acids Res. 31*, 3406–3415.
35. Sakuragi, J., Sakuragi, S., and Shioda, T. (2007) Minimal region sufficient for genome dimerization in the human immunodeficiency virus type 1 virion and its potential roles in the early stages of viral replication. *J. Virol. 81*, 7985–7992.
36. Berkhout, B., Das, A. T., and van Wamel, J. L. (1998) The native structure of the human immunodeficiency virus type 1 RNA genome is required for the first strand transfer of reverse transcription. *Virology 249*, 211–218.
37. Laughrea, M., and Jetté, L. (1994) A 19-nucleotide sequence upstream of the 5′ major splice donor is part of the dimerization domain of human immunodeficiency virus 1 genomic RNA. *Biochemistry 33*, 13464–13474.

BI7023173